ADVANCED FUNCTIONAL MATERIALS

Supporting Information

for

Advanced Functional Materials, adfm.200600022

Supporting information

: For the manuscript entitled with "**Heterostructured Visible Light Active Photocatalyst of Chromia Nanoparticle–Layered Titanate**" by *Tae Woo Kim, Su Gil Hur, Seong-Ju Hwang*, Hyunwoong Park, Wonyong Choi, and Jin-Ho Choy*

1. XRD results for CrO_x–$Ti_{1.83}O_4$ nanohybrid synthesized by an ion-exchanged method and its calcined derivatives

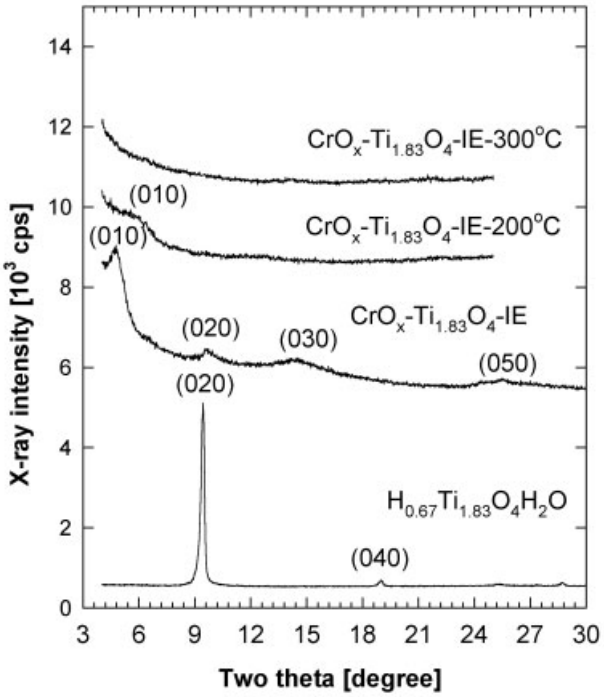

Figure S1. Powder XRD patterns of the protonic titanate and the CrO_x–$Ti_{1.83}O_4$ nanohybrid prepared by an ion-exchange reaction and its derivatives calcined at 200 and 300 °C for 2 h.

The present XRD results reveal that the chromia–titanate heterostructure can also be formed via an ion-exchange method. However, the resulting pillared compound was determined to be fairly weak in thermal stability, since its layered structure started to collapse at as low a temperature as 200 °C.

2. TGA results

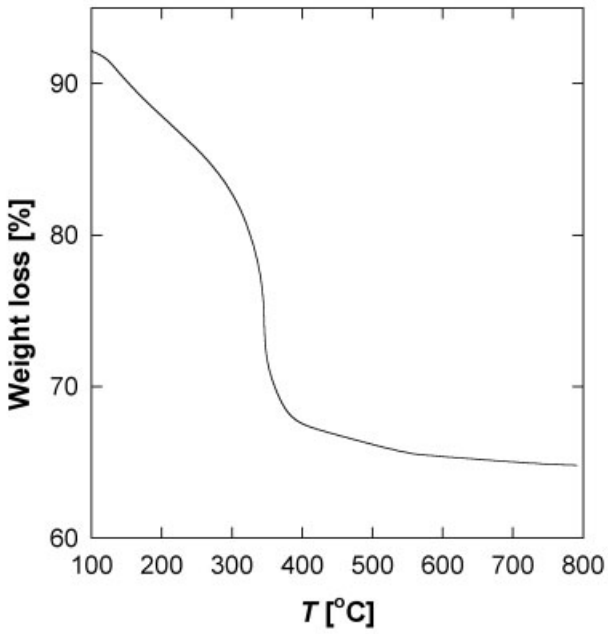

Figure S2. TGA curves of the as-prepared CrO_x–$Ti_{1.83}O_4$ nanohybrid under ambient atmosphere.

: The thermal behavior of the CrO_x–$Ti_{1.83}O_4$ nanohybrid was probed by performing TGA analysis under ambient atmosphere at the rate of 10 °C/min. As shown in the above figure, the present nanohybrid exhibits considerable weight losses below 400 °C. A slow weight decrease in the temperature range of 100–320 °C is attributable to the dehydration and the dehydroxylation of chromia cluster in the interlayer space. The decomposition of organic acetate group in the interlayer chromia cluster is responsible for the abrupt weight loss in higher temperature region. No marked weight loss occurs beyond 400 °C, indicating the complete thermal decomposition of the interlayer chromia cluster below this temperature.

3. FE-SEM results

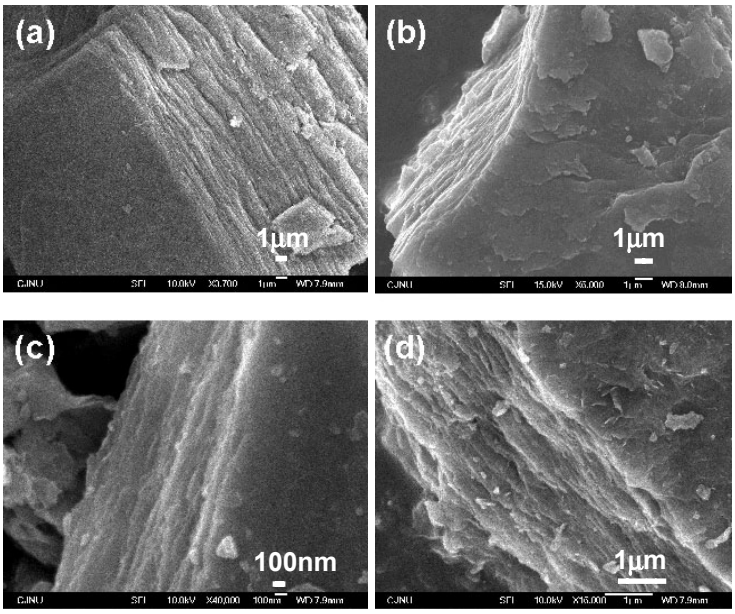

Figure S3. FE-SEM images for a) the as-prepared CrO_x–$Ti_{1.83}O_4$ nanohybrid and its derivatives calcined at b) 200, c) 300, and d) 500 °C for 2 h.

The morphologies of the as-prepared CrO_x–$Ti_{1.83}O_4$ nanohybrid and its calcined derivatives were monitored by FE-SEM analysis. The images of the regular stacks of titanate sheets are common for the as-prepared chromia–titanate nanohybrid and its calcined derivatives. This observation indicates that the titanate sheets and chromia particles in these samples are well ordered in layer-by-layer restacking. In the FE-SEM image of the calcined derivative at 500 °C, the overall stacks of layered titanate crystallites are maintained with a partial collapse of pillared structure.

4. Ti K-edge XANES results

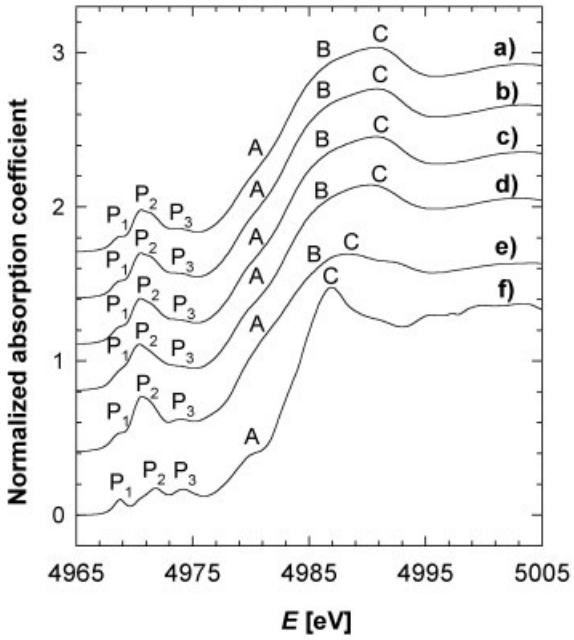

Figure S4. Normalized Ti K-edge XANES spectra for a) the as-prepared CrO_x–$Ti_{1.83}O_4$ nanohybrid and its derivatives calcined at b) 200 °C, c) 300 °C, and d) 500 °C for 2 h, in comparison with the reference spectra for e) $Cs_{0.67}Ti_{1.83}O_4$ and f) TiO_2.

The Ti K-edge XANES spectra for the as-prepared CrO_x–$Ti_{1.83}O_4$ and its calcined derivatives are plotted in the above figure, in comparison with those for the reference cases of TiO_2 and the pristine $Cs_{0.67}Ti_{1.83}O_4$. All the spectra presented here show three pre-edge peaks (denoted P_1, P_2, P_3), which correspond to the transitions from core 1s level to unoccupied 3d states. It was well-known that the intensity and energy of the peak P_2 reflect sensitively the local atomic arrangement of titanium ions. That is, as the local structure of titanium ion is more distorted from regular octahedron, this peak P_2 becomes stronger and moves toward lower energy side. Except slight intensity difference, spectral features in pre-edge region appear nearly the same for both the pristine cesium titanate and the chromia–titanate nanohybrid, indicative of little change of Ti local structure before and after the hybridization. In main-edge region, there are three spectral features (denoted A, B, and C) corresponding to the dipole-allowed 1s → 4p transitions. In the case of CrO_x–$Ti_{1.83}O_4$, the overall spectral feature in main-edge region is rather similar to that of the pristine cesium titanate, underlining that the crystal structure of titanate layer remains nearly the same upon the hybridization with the chromia cluster. Furthermore, no marked spectral change appears after the calcination process.

5. Structural models for various types of chromia oligomers

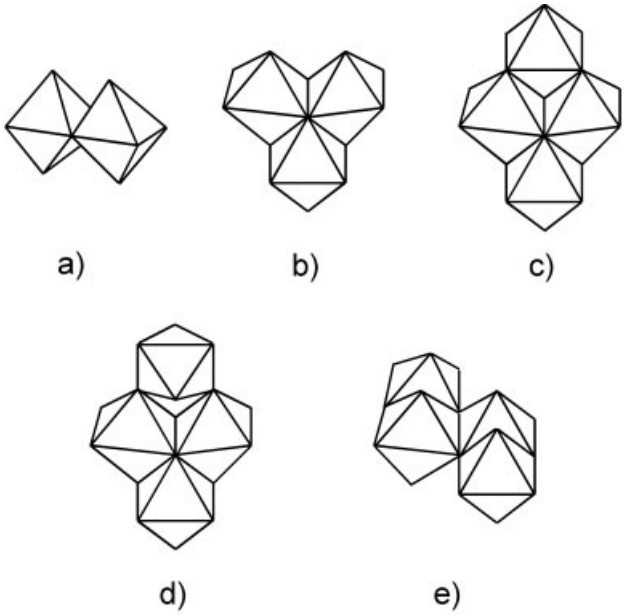

Figure S5. Various types of chromia oligomers formed by the connection of CrO_6 (or $Cr(OH)_6$) octahedra. a) dimer, b) trimer, c) close tetramer, d) open tetramer, and e) zigzag chain of edge-shared CrO_6 octahedra. The octagon represents CrO_6 octahedron.

: Depending on the way of connection among octahedral CrO_6 units, diverse types of oligomers can be formed such as dimeric, trimeric, open tetrameric, and close tetrameric clusters. The above figure represents various types of chromia oligomers formed by the connection of CrO_6 (or $Cr(OH)_6$) octahedra.

6. Photodegradation of AO7 under UV-visible and visible irradiations

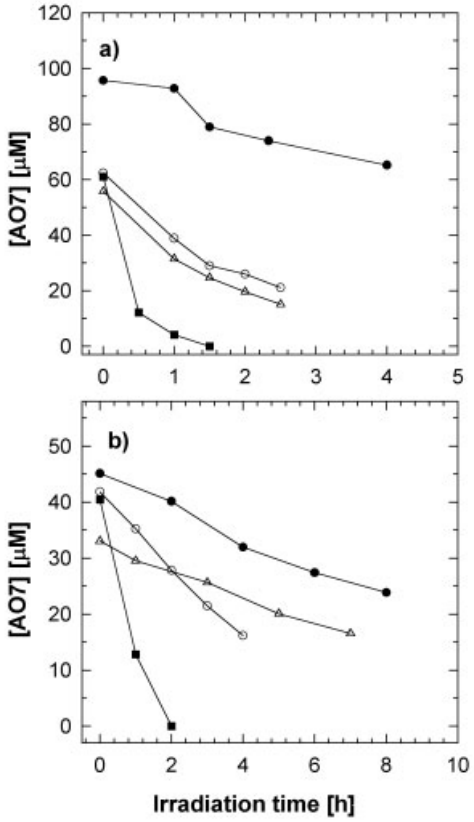

Figure S6. Comparison of photocatalytic degradation time profiles of AO7 in $Cs_{0.67}Ti_{1.83}O_4$ (★), CrO_x–$Ti_{1.83}O_4$-200 °C (▩), CrO_x–$Ti_{1.83}O_4$-300 °C (●), and CrO_x–$Ti_{1.83}O_4$-400 °C (□) suspension under a) UV–visible and b) visible light irradiation. For UV–visible illuminated tests, [photocatalyst] = 0.67 g/L; $[AO7]_0$ = 100 μM; pH_i = 3.0; open to air. For visible light-illuminated tests, [photocatalyst] = 0.5 g/L; $[AO7]_0$ = 50 μM; pH_i = 3.5; open to air.

The variation of AO7 concentration during the photoreaction is plotted as a function of irradiation time in the above figure. Under both conditions of UV–visible (λ > 300 nm) and visible (λ > 420 nm) alone irradiation, the CrO_x–$Ti_{1.83}O_4$ nanohybrids exhibited higher activities for AO7 degradation than the pristine layered titanate. Such an improvement of photocatalytic activity after the hybridization is surely due to the presence of visible light harvestable CrO_x species in the interlayer space of layered titanate, leading to the utilization of visible photon energy to photoreaction.

7. Wave length dependence of photodegradation of 4-CP

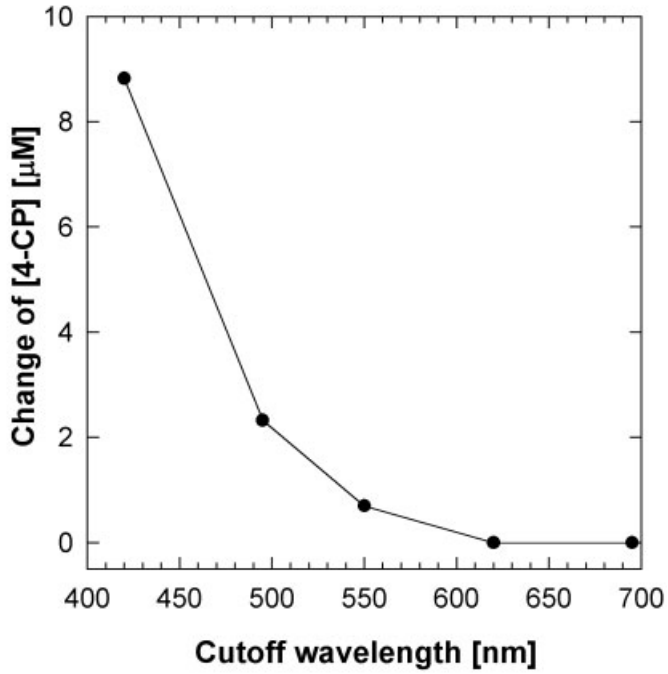

Figure S7. Wavelength dependence of photocatalytic degradation of 4-CP in visible light-illuminated suspensions of CrO_x–$Ti_{1.83}O_4$-400 °C nanohybrid. [photocatalyst] = 0.5 g/L; $[4\text{-CP}]_0$ = 100 μM; pH_i = 4.0; reaction time = 4 hr; open to air.

: In order to verify the effect of hybridization on the active wavelengths of the titanate, we investigated the degradation of 4-CP as a function of the irradiation wavelength that was varied by a set of cutoff filters. As plotted in the above figure, 4-CP was clearly decomposed under visible light irradiation up to the cutoff wavelength of ~500 nm. This value matches well with the measured bandgap energy of the nanohybrids. This result provides clear evidence that the visible light driven photocatalytic activity of the nanohybrid is surely due to the coupling between chromia and titanate species.